MPP5 Recruits MPP4 to the CRB1 Complex in Photoreceptors

Albena Kantardzhieva,[1,2] *Ilse Gosens,*[2,3] *Svetlana Alexeeva,*[1] *Ingrid M. Punte,*[3] *Inge Versteeg,*[1] *Elmar Krieger,*[4] *Carla A. Neefjes-Mol,*[1] *Anneke I. den Hollander,*[3] *Stef J. F. Letteboer,*[3] *Jan Klooster,*[1] *Frans P. M. Cremers,*[3] *Ronald Roepman,*[3] *and Jan Wijnholds*[1]

Purpose. Mutations in the human Crumbs homologue 1 (*CRB1*) gene are a frequent cause of Leber congenital amaurosis (LCA) and various forms of retinitis pigmentosa. CRB1 is thought to organize an intracellular protein scaffold in the retina that is involved in photoreceptor polarity. This study was focused on the identification, subcellular localization, and binding characteristics of a novel member of the protein scaffold connected to CRB1.

Methods. To dissect the protein scaffold connected to CRB1, the yeast two-hybrid approach was used to screen for interacting proteins. Glutathione *S*-transferase (GST) pull-down analysis and immunoprecipitation were used to verify protein–protein interactions. The subcellular localization of the proteins was visualized by immunohistochemistry and confocal microscopy on human retinas and immunoelectron microscopy on mouse retinas.

Results. A novel member of the scaffold connected to CRB1, called membrane palmitoylated protein (MPP) subfamily member 4 (MPP4), a membrane-associated guanylate kinase (MAGUK) protein, was identified. MPP4 was found to exist in a complex with CRB1 through direct interaction with the MPP subfamily member MPP5 (PALS1). 3D homology modeling provided evidence for a mechanism that regulates the recruitment of both homo- and heterodimers of MPP4 and -5 proteins to the complex. Localization studies in the retina showed that CRB1, MPP5, and MPP4 colocalize at the outer limiting membrane (OLM).

Conclusions. These data imply that MPP4 and -5 have a role in photoreceptor polarity and, by association with CRB1, pinpoint the cognate genes as functional candidate genes for inherited retinopathies. (*Invest Ophthalmol Vis Sci.* 2005;46:2192–2201) DOI:10.1167/iovs.04-1417

The polarized organization of photoreceptor cells is a fundamental feature of the developing retina. Polarity can be either a dynamic event during which proteins are shuttled across the cell or a more static process in which proteins are clustered in complexes and retained at particular subcellular locations.[1,2] Detailed studies of the factors that play a role in this site-specific localization could provide knowledge about the general pathways that establish and maintain retinal polarity. It can also help us to understand the pathologic pathways in the retina that are triggered by mutations in genes that encode components of such complexes.

Several members of the membrane associated guanylate kinase (MAGUK) protein family are involved in cell polarity through their role in large multiprotein complexes at tight junctions.[3,4] This protein family is characterized by a specific set of protein-binding domains, consisting of one or more PDZ (postsynaptic density 95/discs large/zonula occludens 1) domains, an SH3 (Src homology 3) domain, and a region with homology to a guanylate kinase (GuK) domain.[5,6] Some members, such as PALS1 (assigned the name MPP5 by the HUGO Gene Nomenclature Committee; gene.ucl.ac.uk/nomenclature; hosted by the University College London, London, UK), ZO1, and PSD-95, have been shown to be localized at sites of cell–cell contact (e.g., synapses and epithelial tight junctions).[7–10] It is currently assumed that MAGUK proteins serve as scaffolds by recruitment of other MAGUKs, eventually linking them to the cell cytoskeleton or to the carboxyl terminus of transmembrane proteins.[3,11,12]

The MAGUK protein Stardust is the *Drosophila* homologue of MPP5, one of the seven mammalian membrane palmitoylated protein (MPP) subfamily members. Stardust mutants exhibit severe disruption in apicobasal polarity in embryonic epithelia.[13] In addition, mutants of the zebra fish homologue *Nagie oko* display severe defects in the organization of the retinal cell layers,[14] and loss of Stardust gives rise to an eye phenotype in *Drosophila* characterized by a shortened stalk membrane and altered rhabdomere morphogenesis resembling the Crumbs mutant phenotype.[15–17]

Crumbs is an apically localized transmembrane protein involved in organizing the apical plasma membrane subdomains.[18–21] Stardust has been found to colocalize with Crumbs and interact physically with the C-terminal ERLI motif of Crumbs through its PDZ domain.[22] This interaction was recently also identified for their mammalian homologues MPP5 and CRB1[10] as well as for MPP5 and CRB3.[23] Stardust and Crumbs are both necessary to ensure stability, localization, and function in controlling the apicobasal polarity of epithelial cells.[18,22] The Crumbs-Stardust protein complex also recruits the *Drosophila* protein associated with tight junctions (DPATJ; formerly known as Discs lost). This cytoplasmic multi-PDZ domain protein interacts indirectly, via Stardust, with the cy-

From [1]The Netherlands Ophthalmic Research Institute, Amsterdam, The Netherlands; the [3]University Medical Centre Nijmegen, Nijmegen, The Netherlands; and the [4]Centre for Molecular and Biomolecular Informatics, Nijmegen, The Netherlands.

[2]Contributed equally to the work and should therefore be considered equivalent authors.

Supported in part by Grant QLG3-CT-2002-01266 from the European Commission (EC), Grant 912-02-018 from the Netherlands Organization for Scientific Research (JW, FPMC), and Grant N-CB-0600-0003 from the Foundation Fighting Blindness (FPMC, AIdH).

Submitted for publication December 3, 2004; revised January 25, 2005; accepted January 26, 2005.

Disclosure: **A. Kantardzhieva**, None; **I. Gosens**, None; **S. Alexeeva**, None; **I.M. Punte**, None; **I. Versteeg**, None; **E. Krieger**, None; **C.A. Neefjes-Mol**, None; **A.I. den Hollander**, None; **S.J.F. Letteboer**, None; **J. Klooster**, None; **F.P.M. Cremers**, None; **R. Roepman**, None; **J. Wijnholds**, None

The publication costs of this article were defrayed in part by page charge payment. This article must therefore be marked "*advertisement*" in accordance with 18 U.S.C. §1734 solely to indicate this fact.

Corresponding author: Jan Wijnholds, The Netherlands Ophthalmic Research Institute, Meibergdreef 47, 1105 BA, Amsterdam, The Netherlands; j.wijnholds@ioi.knaw.nl.

TABLE 1. Sense and Antisense Primer Sequences for GATEWAY Constructs

Construct (aa position)	Sense	Antisense
bCRB1^{intra} (1372-1408)	5′-TCGCCTCCAACAAAAGGGCAAC-3′	5′-CCTAGATCAGCCTCTCTGCTGCAG-3′
hCRB1^{intra} (1369-1406)	5′-TCACCTCCAACAAAAGGGCAACTCA-3′	5′-CCTAAATCAGTCTCTCCATTGC-3′
hMPP5^{FL} (1-675)	5′-ATGACAACATCCCATATGAAT-3′	5′-TCACCTCAGCCAAGTGGATGG-3′
hMPP5^{SH3+HK} (377-477)	5′-CAGATCAAGCCGCCTCCTG-3′	5′-CTTCCTATTTGCTGGCTGATG-3′
hMPP5^{PDZ} (237-348)	5′-TTACAGATGAGAGAGTTTATGAAAG-3′	5′-GGATTACTGTTTCCTTGGCAGG-3′
hMPP5^{CC} (1-122)	5′-ATGACAACATCCCATATGAATG-3′	5′-TAATATTTTCACAGCATAATGAGG-3′
hMPP5^{GuKc} (470-675)	5′-CTTTATCATCAGCCAGCAAATAGG-3′	5′-TCACCTCAGCCAAGTGGATGG-3′
hMPP5^{HK-end} (408-675)	5′-CCAGGGAAAAGCTTTCAGCAGC-3′	5′-TCACCTCAGCCAAGTGGATGG-3′
hMPP4^{FL} (1-637)	5′-ATGATACAGTCAGACAAAGGAG-3′	5′-TCATTGAGACTCAGTATCTG-3′
hMPP4^{SH3+HK} (245-425)	5′-GTGTACGTCCGTGCCATGAC-3′	5′-GTCTATGACTCAGAGTTACT-3′
hMPP4^{PDZ} (141-244)	5′-TGCCAGACAATATCCCTGAGAG-3′	5′-CCATCTGCTGGCTATTCACAGG-3′
hMPP4$^{SH3-end}$ (245-637)	5′-GTGTACGTCCGTGCCATGAC-3′	5′-TCATTGAGACTCAGTATCTG-3′
hMPP4$^{Edom-end}$ (410-637)	5′-GGTGCCCCTTACGAGGAGG-3′	5′-TCATTGAGACTCAGTATCTG-3′
hMPP4$^{365-637}$ (365-637)	5′-GAGGAGTTTGTTGGCTACGG-3′	5′-TCATTGAGACTCAGTATCTG-3′

toplasmic tail of Crumbs. These three proteins colocalize in *Drosophila* photoreceptors during and after eye development.[17] The mammalian CRB1-MPP5-PATJ complex localizes to tight junctions where it may control cell polarity.[10] In the mouse retina, the CRB1-MPP5-PATJ proteins colocalize at the apical region adjacent to adherens junctions of photoreceptors.[24] The *Drosophila* Crumbs protein and the human homologue CRB1 are 35% similar in amino acid sequence and contain the same conserved protein motifs.[25] Mutations have been identified in the *CRB1* gene in individuals with Leber congenital amaurosis (LCA); retinitis pigmentosa (RP) type 12, with preservation of para-arteriolar retinal pigment epithelium (PPRPE); RP with Coats-like exudative vasculopathy; and early-onset RP without PPRPE.[26–29] CRB1 has been found to maintain adherens junctions between photoreceptor cells and Müller glia cells,[30] thus preventing delamination of the photoreceptor layer and death of retinal neurons.[24,31]

In this study we identified a second MPP subfamily member, MPP4, existing in a complex with CRB1 through direct interaction with MPP5. The presence of MPP4 and -5 in this CRB1 protein complex implicates these proteins in photoreceptor polarity and putatively in inherited retinal dystrophies.

MATERIALS AND METHODS

DNA Constructs

Human retinal cDNA (Marathon Ready; BD-Clontech, Palo Alto, CA) or mouse B6D2 retinal cDNA synthesized with a cDNA amplification kit (Marathon; BD-Clontech), was used to amplify the full-length cDNAs for human *CRB1*, *MPP5*, *MPP4*, and mouse *Mpp4* with a cDNA PCR kit (Advantage; Clontech). For human *CRB1* the following primers were used: 5′-GGGATCCAAATACCACC*ATG*GCACTTAAGAACATTAACTAC-3′ (sense) and 5′-GATCCTCGAGTC*CTA*AATCAGTCTCTCCATTGCAGG-3′ (antisense). Italic sequences denote start and stop codons of the gene. Two consecutive Myc tags were inserted at amino acid (aa) position 1331 with the following primers: 5′-GCGAACAAAAACTCATCTCAGAAGAGGATCTG-3′ (sense), and 5′-GCAGATCCTCTTCTGAGATGAGTTTTTGTTC-3′ (antisense). The human *MPP5* PCR was performed with primers 5′-GATCCCGGGCCATC*ATG*ACAACATCCCATATGAATGGGCATG-3′ (sense) and 5′-GATCGTCGAC*TCA*CCTCAGCCAAGTGGATGGTAC-3′ (antisense). Human *MPP4* was synthesized with primers 5′-GATCCCGGGCCATC*ATG*ATACAGTCAGACAAAGGAGCAG-3′ (sense) and 5′-GATCGTCGAC*TCA*TTGAGACTCAGTATCTGAG-3′ (antisense), and mouse *Mpp4* with 5′-GATCCCGGGCCATC*ATG*AGACAGTCTGACAGAGGAGCAG-3′ (sense) and 5′-GATCGTCGAC*TTA*AGATTCAGTGTCAGGGGAAACC-3′ (antisense). A 3xFLAG epitope tag was created at the N terminus of human *MPP4* with the following primers 5′-GACTACAAAGACCATGACGGTGATTATAAAGATCATGACATCG-ATACAAGGATGACGATGACAAGCTCATG-3′ (sense), and 5′-GTACAGCTTGTCATCGTCATCCTTGTAATCGATGTCATGATCTTTATAATCACCGTCATGGTCTTTGTAGTC-3′(antisense).

The following constructs were made by PCR using the a cloning system (Gateway; Invitrogen, Groningen, The Netherlands), according to the manufacturer's procedures, using full-length constructs as a template: the intracellular domains of bovine CRB1 (bCRB1^{intra}) and human CRB1 (hCRB1^{intra}); the full-length human MPP5 (MPP5^{FL}); the SH3 and HOOK domains of human MPP5 (MPP5^{SH3+HK}); the C terminus of human MPP5 from the HOOK domain (MPP5^{HK-end}); the PDZ domain of human MPP5 (MPP5^{PDZ}); the coiled-coil domain of human MPP5 (MPP5^{CC}); the GuK domain of human MPP5 (MPP5^{GuK}); full-length human MPP4 (MPP4^{FL}); the PDZ domain of human MPP4 (MPP4^{PDZ}); the C terminus of MPP4 containing the E domain and GuK domain (MPP4$^{Edom-end}$); the C terminus of MPP4 (MPP4$^{365-637}$); the SH3 and HOOK domains of human MPP4 (MPP4^{SH3+HK}); and the C terminus of MPP4 from the SH3 domain (MPP4$^{SH3-end}$). Gene-specific primers that were used to make these constructs are listed in Table 1. The attB1 and attB2 linkers were attached to the 5′ end of, respectively, the sense and antisense primers.

The commercially adapted destination vectors pBD-GAL4/DEST and pAD-GAL4/DEST (Gateway; Invitrogen) were created by insertion of the blunt-ended reading frame (Rf) cassette B into, respectively, the *Eco*RI and *Sal*I sites of pBD-GAL4-2.1-Cam (Stratagene, Amsterdam, The Netherlands) and the *Bam*HI and *Sal*I sites of pAD-GAL4-2.1 (Stratagene),[32] with sticky ends previously filled in using Klenow (Invitrogen). The destination vectors pDest-15 (N-GST fusion tag) and pDest-17 (N-6xHis fusion tag) were purchased from Invitrogen. The pDest566 was constructed by introduction of a reading frame cassette (Gateway; Invitrogen) into a modified version of pET-43a (Novagen, Madison, WI) containing an amino terminal His6-maltose-binding protein tag (Esposito D, Hartley J, unpublished data, 2003). All novel constructs were verified by nucleotide sequencing.

Yeast Two-Hybrid

A GAL4-based yeast two-hybrid system (Hybrizap; Stratagene), with yeast strain PJ69-4α, was used to identify proteins that interact with CRB1^{intra} and MPP5. The pBD-hMPP5^{CC}, pBD-hMPP5^{GuK}, and pBD-hMPP5^{SH3+HK} constructs were used as baits on an oligo-dT primed human retina cDNA library, representing 2.1×10^6 primary cDNA clones. In total, 8.2×10^5, 1×10^6, and 6.8×10^5 clones were plated, respectively. The human and bovine pBD-CRB1^{intra} constructs were used to screen respectively a pretransformed oligo-dT primed human and a randomly primed bovine retina cDNA library by yeast cell-to-cell mating, resulting in screening 1.0×10^7 and 1.4×10^7 clones.[33] In subsequent yeast two-hybrid experiments, different domains of MPP5 and -4 were tested for interaction by cotransformation into the YRG-2 yeast strain. Interactions were quantified in a liquid ortho-nitrophenyl-β-D-galactopyranoside (ONPG) assay for β-galactosidase activity.[34]

Antibodies

Bacterially expressed full-length MPP5 protein was used for immunization of chicken. The yolk was processed with an IgY Purification Kit (Eggcellent Chicken; Pierce Biotechnology, Rockford, IL) according to the manufacturer's protocol, and IgY antibodies were consequently affinity purified on a protein-coupled NHS-activated HP column (HiTrap; Amersham Biosciences, Roosendahl, The Netherlands).

Production of AK2, AK5, AK7, AK4, and AK8 antibodies have been described.[24] Anti-c-*myc* monoclonal mouse antibodies (clone 9E10) were purchased from Roche; anti-rat MUPP1 (clone 43) and anti-β-catenin (clone 14) mouse monoclonal antibodies from BD Biosciences (Leiden, The Netherlands); anti-6x His antibody from Santa Cruz Biotechnology (Heerhugowaard, The Netherlands); anti-FLAG monoclonal mouse antibody (clone M2), monoclonal anti-chicken IgG (clone CG-106), and rat monoclonal anti-uvomorulin (clone Decma-1) from Sigma-Aldrich (Amsterdam, The Netherlands). Secondary antibodies conjugated to Alexa 488, Cy3, and Cy5 were obtained from Molecular Probes (Leiden, The Netherlands) and Jackson ImmunoResearch Laboratories (West Grove, PA). Secondary antibodies conjugated to horseradish peroxidase, were purchased from Sigma-Aldrich and Zymed (Uden, The Netherlands).

Cell Culture

Human embryonic kidney (293HEK) and Madin-Darby canine kidney type II (MDCKII) cells were grown in DMEM (Invitrogen) containing 1% penicillin/streptomycin and 10% fetal bovine serum. Stably transfected MDCKII/CRB1 clones were generated by transduction of MDCKII cells with pBABE-CMV-Puro-*CRB1* retroviruses, and subsequently selected with 2 μg/mL puromycin.

GST Pull-Down, Coimmunoprecipitation, and Western Blot Analysis

Arabinose inducible BL21-AI cells were transformed with GST-hCRB1^{intra}/pDest15, or His-MBP-hMPP5^{PDZ}/pDest566 and IPTG-inducible BL21-DE3 cells with GST-hMPP5^{SH3+HK}/pDest15 or His-MBP-hMPP4$^{HK\text{-}end}$/pDest566. BL21-DE3 cell lysates were prepared according to a 1.5% sarkosyl protocol with DNase added before centrifugation.[35] BL21-AI cell lysates were prepared (B-PER; Pierce Biotechnology, Etten-Leur, The Netherlands), with a protease inhibitor cocktail (Roche, Almere, The Netherlands) plus 1 μg/mL pepstatin A and 5 mM dithiothreitol (DTT). For GST pull downs, equal amounts of blocked (1.5 mg/mL BSA) glutathione Sepharose beads (4B; Amersham Pharmacia, Uppsala, Sweden) with glutathione *S*-transferase (GST), beads with GST fusion proteins, or beads alone were incubated with 0.5 mL of lysates containing His-MBP-fusion proteins for 2 hours at 4°C. After several washes with lysis buffer and TBS containing 1% Triton X-100 and 2 mM DTT, the beads were boiled, and proteins were resolved on SDS-polyacrylamide gels.

For coimmunoprecipitation experiments, 293HEK cells were transfected with pBabe-CMV-Puro/Hygro-CRB1/MPP5/MPP4, with a commercial reagent (Fugene 6; Roche) or calcium phosphate. After 48 hours, cells were lysed in 50 mM HEPES (pH 7.4), 150 mM sodium chloride, 10% glycerol, 0.5% Triton X-100, 1.5 mM magnesium chloride, 1 mM EGTA, 1 mM phenylmethylsulfonyl fluoride (PMSF), a protease inhibitor cocktail (Roche), and 10 μg/mL aprotinin (Sigma-Aldrich). Either protein LA-agarose (Sigma-Aldrich) was used to bind the primary antibodies after incubation of precleared supernatants with 10 to 15 μg antibody for 4 to 16 hours at 4°C, or antibodies were precoupled to protein G beads (Dynabeads; Dynal Biotech ASA, Oslo, Norway) before incubation of supernatants for 2 hours at 4°C. For immunoprecipitation with anti-MPP5 antibody SN47, mouse monoclonal anti-chicken IgG was precoupled to the protein G beads (15 μg/reaction), followed by a second round of coupling of chicken anti-MPP5 antibody SN47 (10 μg/reaction) and incubation with cell lysates for 2 hours at 4°C. The beads were washed three times in 10% glycerol/PBS or lysis buffer, respectively and boiled in sample buffer with β-mercaptoethanol, and the immunocomplexes were resolved by SDS-PAGE. For Western blot analyses, proteins were electrophoretically transferred onto nitrocellulose membranes, which were then blocked, incubated with primary and secondary antibodies (conjugated to horseradish peroxidase) in 0.3% to 5% milk powder/TBS, and washed in TBS. The bands were visualized with a chemiluminescence reagent (ECL; Amersham Biosciences).

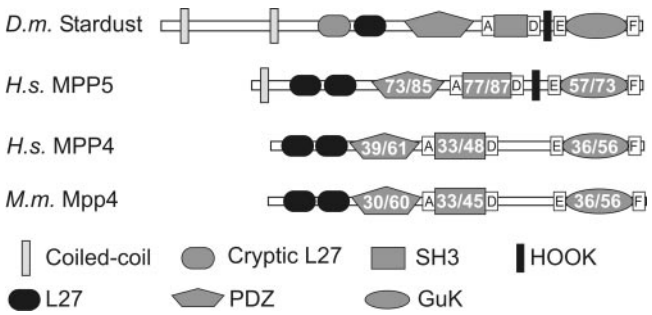

FIGURE 1. Alignment of Stardust homologues. Stardust was individually aligned with its closest human homologue MPP5 and with human and mouse MPP4. The percentages of identical and similar amino acid sequence of the conserved PDZ, SH3, and GuK domains are shown in the respective boxes. Stardust and MPP5 contain an additional HOOK domain. Strands A and D flanking the SH3 domain and E and F flanking the GuK domain were identified according to homology with PSD-95.

N-Glycosylation Experiments

After they reached 70% confluence, stable clones of MDCKII cells expressing hCRB1 were cultured for 1 to 5 days in DMEM supplemented with 1% penicillin/streptomycin, 10% fetal bovine serum, and 5 μg/mL tunicamycin dissolved in dimethylsulfoxide (DMSO) or only DMSO for the control cells.

Expression Profiles

Total RNA was isolated from different human tissues and from an ARPE-19 cell-line (Dunn KC, et al. *IOVS* 1995;36:ARVO Abstract 766). For the semiquantitative RT-PCR, 3.1 μg RNA was reverse transcribed using random hexanucleotides.[36] A touchdown PCR was performed for 28 and 33 cycles on 62 ng cDNA for CRB1, MPP5, MPP4, and the housekeeping gene GAPDH, which served as a standard. The following primer pairs were used: 5′-ACCAATGTATTCAACAGGGACC-3′(sense) and 5′-TCGTTTCCGTTGTAGTGTCTCC-3′ (antisense) for CRB1, 5′-GTATGGAACTAGCATAGATTCTG-3′ (sense) and 5′-CAAGATCGGAATTCACAATTGCC-3′ (antisense) for MPP5, 5′-CACCTGTATGGCACTAGTGTGG-3′ (sense) and 5′-CATACACCTCATATTCGATGGC-3′ (antisense) for MPP4, and 5′-ACCACAGTCCATGCCATCAC-3′ (sense) and 5′-TCCACCACCCTGTTGCTGTA-3′ (antisense) for GAPDH.

Immunohistochemistry

Eight human postmortem retinas, with enucleation times of 8 to 24 hours, were obtained from the cornea bank in Amsterdam and treated in accordance with the guidelines of the Declaration of Helsinki for the use of human tissue in research.

Frozen human retina sections, 10 μm thick, were treated essentially as described previously[24] using PBS buffer and 1% BSA. Sections were imaged on a confocal laser-scanning microscope (model 501; Carl Zeiss Meditec, Jena, Germany).

Immunoelectron Microscopy

Immunoelectron microscopy on mouse retina sections was performed as described previously.[37] Ultrathin sections were examined and photographed (model 201 electron microscope; Phillips, Eindhoven, The Netherlands).

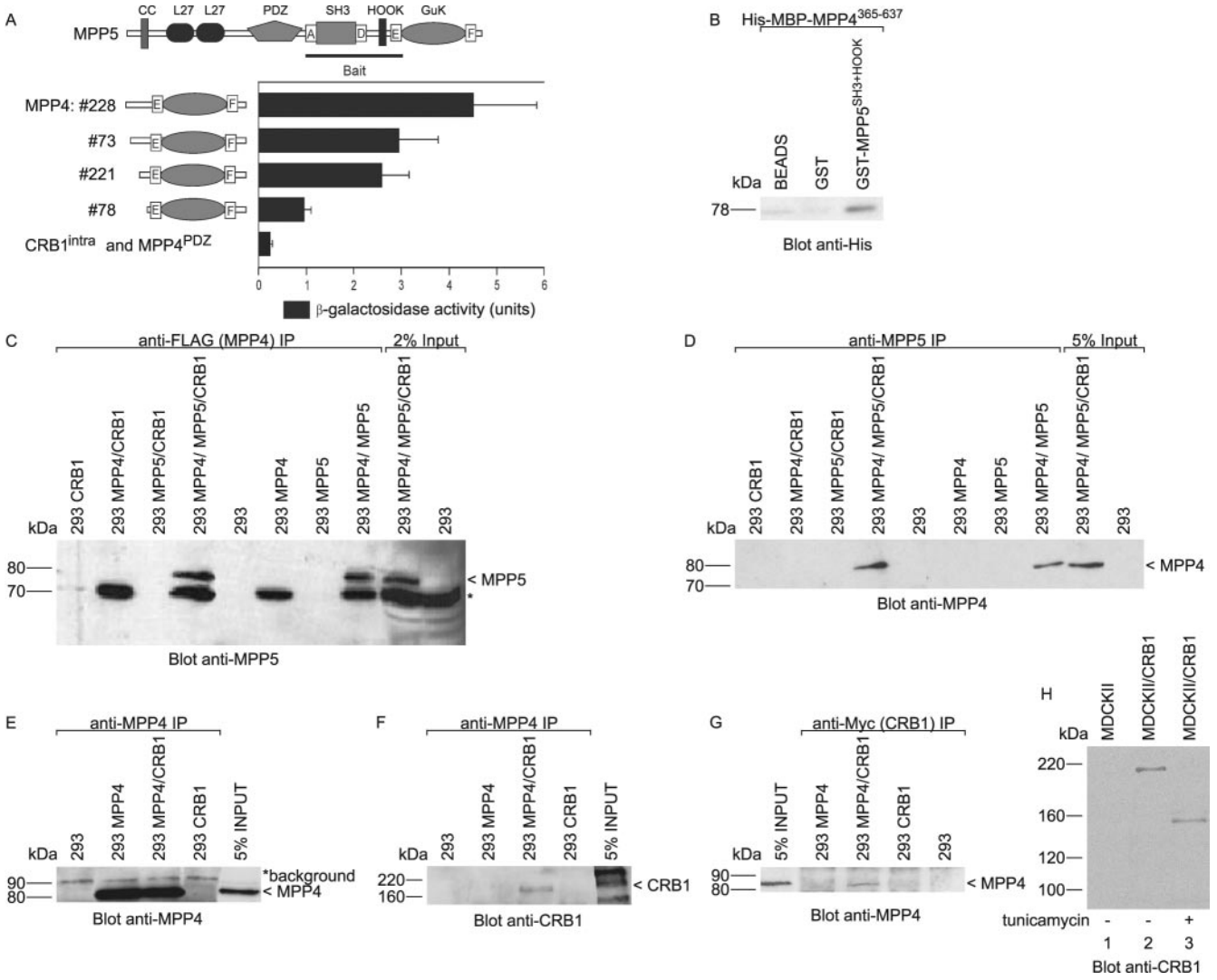

FIGURE 2. Identification and confirmation of interactions between MPP5 and MPP4. (**A**) Determination of the relative binding affinity between MPP5 and -4. YRG-2 yeast cells were cotransformed with the bait (SH3-HOOK region of MPP5) and different clones of MPP4 from the yeast two-hybrid screen. Activation of the *LacZ* reporter gene was determined by a liquid ONPG assay (β-galactosidase activity (■). In this assay, the pBD-GAL4 domain, fused to the intracellular domain of CRB1, which has no binding affinity for the PDZ domain of MPP4, was used as a negative control, showing basal levels of reporter gene activation. (**B**) Interaction between MPP5 and -4 was confirmed in a GST-MPP5^{SH3+HK} pull-down from bacterial lysates expressing His-MBP-MPP4$^{365-637}$. (**C**) Anti-FLAG antibody coimmunoprecipitated MPP5 from cells overproducing 3xFLAG-MPP4 and MPP5, as well as from cells overproducing 3xFLAG-MPP4, MPP5, and CRB1-myc. *Asterisk*: an endogenous 70-kDa form of MPP5, coimmunoprecipitated from all 3xFLAG-MPP4-overexpressing cells. (**D**) Anti-MPP5 antibody (SN47) coimmunoprecipitated MPP4 from cells overproducing 3xFLAG-MPP4 and MPP5, as well as from cells overproducing 3xFLAG-MPP4, MPP5, and CRB1-myc. (**E**) The anti-MPP4 antibody (AK4) immunoprecipitated MPP4 from cells overproducing 3xFLAG-MPP4 or CRB1-myc and 3xFLAG-MPP4. *Asterisk*: an unspecific band of 92 kDa. (**F**) Anti-MPP4 antibody (AK4) coimmunoprecipitated CRB1-myc from cells overproducing CRB1-myc and 3xFLAG-MPP4. (**G**) Anti-myc antibody coimmunoprecipitated 3xFALG-MPP4 from cells overproducing CRB1-myc and 3xFLAG-MPP4. (**H**) N-glycosylation of CRB1. Incubation of stable MDCKII/CRB1 cells with tunicamycin shifted the molecular weight from more than 220 kDa toward the calculated 154 kDa, indicating extensive N-glycosylation of CRB1.

Molecular Modeling of MPP4 and -5

The amino acid sequences of MPP4 (Swiss Prot accession number Q96JB8; http://www.expasy.org; provided in the public domain by Swiss Institute of Bioinformatics, Geneva, Switzerland) and MPP5 (accession number Q8N3R9) were submitted to the 3D-PSSM fold recognition server[38] to search the protein data base (PDB) for homology modeling templates. The best hit in both cases (E-value 0.07) was PDB file 1KJW, the SH3-GuK module of Postsynaptic Density Protein 95 (PSD-95), solved at 1.8-Å resolution.[39] With ~40% sequence identity in the aligned regions, the modeling template PSD-95 can be expected to be very similar to the target structures,[40] except for structurally divergent loop regions. Consequently, homology models for MPP4 and -5 were built with What If,[41] using a backbone-dependent rotamer library[42] (see Fig. 3B, left side). Flexible HOOK residues (blue in Fig. 3B) were deleted, and the independent SH3 and GuK domains of MPP4 and -5 were arranged in all four possible permutations. Finally, the side-chain rotamers at the domain interface were optimized with YASARA (Yasara Biosciences, http://www.yasara.org/index.html) by minimizing the NOVA force field energy.[43] The parameters of the NOVA energy function have been optimized based on known high-resolution x-ray structures, so that the function has stable minima as close as possible to these structures. The relative domain-binding energies of the four models were then calculated as described previously.[44] Coordinate files of the models are available from the authors on request.

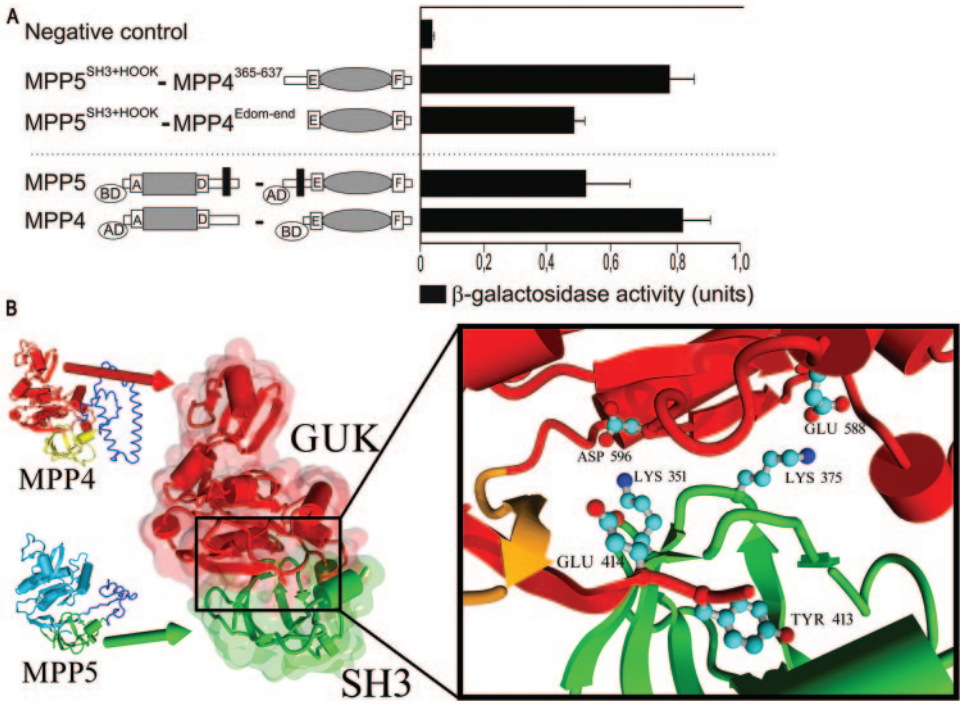

FIGURE 3. Analysis of the interacting domains of MPP4 and -5. (**A**) For quantification of the intermolecular interaction between MPP4 and -5 (*above dotted line*), the YRG-2 yeast strain was cotransformed with the SH3-HOOK region of MPP5, together with two different deletion constructs of MPP4. The minimal region of MPP4 that is needed for interaction contains the E-GuK-F region. For determination of the intramolecular interaction of MPP5 as well as MPP4 (*below dotted line*), yeast cells were cotransformed with two constructs of MPP5 (the pBD-GAL4 domain fused to the SH3-HOOK region and the pAD-GAL4 domain fused to the HOOK-GuK domain), as well as two constructs of MPP4 (the pBD-GAL4 domain fused to the GuK domain and the pAD-GAL4 domain fused to the SH3 domain). Interactions were quantified by determining the activation of the LacZ reporter gene in a liquid ONPG assay (β-galactosidase activity, ■). As a negative control, the pBD-GAL4 domain, fused to $CRB1^{intra}$, and the pAD-GAL4 domain, fused to $MPP4^{PDZ}$, was used. (**B**) Homology modeling of MPP4 and -5. The initial models are shown on the *left*, covering the SH3 (*yellow*, *green*) and GuK domains (*red*, *light blue*). By swapping the domains, one obtains a heterodimer, half of which is shown in the *middle*: the SH3 domain of MPP5 bound to the GuK domain of MPP4. Energy calculations predicted a high binding energy for this interaction (Table 2), due to several salt bridges, shown in the close-up (*right*): the triad Glu 414_{MPP4}-Lys 351_{MPP5}-Asp 596_{MPP4}, Lys 375_{MPP5}-Glu 588_{MPP4}, and (not shown) Arg 418_{MPP4}-Glu 395_{MPP5}. Note that an essential tyrosine (Y413) in the GUK domain of MPP4 is present in the core of the SH3 domain of MPP5.

RESULTS

Screening for Interaction Partners of $CRB1^{intra}$

The conserved putative PDZ and FERM protein-binding regions in the intracellular domain of CRB1 suggest target epitopes for different interactions in this relatively small domain. Therefore, we used this domain as a bait to screen bovine and human yeast two-hybrid retina cDNA libraries. We identified only MPP5 as an interacting protein from the bovine randomly primed library (13 clones out of 1.4×10^7 cotransformants analyzed). A highly saturated screen of the human oligo-dT-primed retina cDNA library (1.0×10^7 cotransformants analyzed) did not reveal any interactors.

Identification of a Novel Interactor with MPP5

Although the MAGUK proteins in general and the MPP family of proteins in particular contain different conserved putative protein–protein interaction domains that allow the buildup of a scaffold, only a few of these domains in MPP5 have known ligands (Fig. 1). We used the conserved epitopes of human MPP5, for which no partners have yet been identified, as baits in yeast two-hybrid screens of a human oligo-dT-primed retina cDNA library. We did not identify interactors for the coiled-coil domain (amino acid [aa] 1-122) nor for the GuK domain (aa 470-675; data not shown). However, a bait construct containing the SH3-HOOK region of human MPP5 was found to interact with MPP4. Four different clones containing the C terminus of MPP4 were identified, with the GuK domain flanked by strands E and F (Fig. 1), starting at aa 319 (#228), aa 365 (#73), aa 368 (#221) and aa 390 (#78) (Fig. 2A). The binding affinities of these different clones for MPP5 were measured semiquantitatively in a liquid *ortho*-nitrophenyl-β-D-galactopyranoside (ONPG) assay, revealing that the peptide stretch of MPP4 containing the regions E, GuK, and F is essential for the interaction. However, when more amino acids were present at the N terminus, the binding affinity increased.

Association of MPP4 and -5 In Vitro and In Vivo

The interaction between MPP4 and -5 was confirmed in a GST pull-down assay (Fig. 2B). GST-$MPP5^{SH3+HK}$ fused to glutathione-Sepharose efficiently pulled down His-MBP-$MPP4^{365-637}$ (Fig. 2B).

Furthermore, to test for a physical interaction between MPP4 and -5 in the presence or absence of CRB1, we used 293HEK cells overexpressing MPP4, and/or MPP5, and/or CRB1 in immunoprecipitation experiments (Figs. 2C–D). Anti-FLAG antibody coimmunoprecipitated MPP5 from cells overproducing 3xFLAG-MPP4 and MPP5, as well as from cells overproducing 3xFLAG-MPP4, MPP5, and CRB1 (Fig. 2C). The 80-kDa recombinant and the endogenously expressed 70-kDa MPP5 coimmunoprecipitated with MPP4 (Fig. 2C). In a reciprocal experiment, anti-MPP5 antibody SN47 coimmunoprecipitated MPP4 from cells overproducing 3xFLAG-MPP4 and MPP5, as well as from cells overproducing 3xFLAG-MPP4, MPP5, and CRB1 (Fig. 2D). Coimmunoprecipitation of MPP4 or CRB1 with immunoprecipitated endogenous 70- and 80-kDa MPP5 was below detection levels (Fig. 2D, and data not shown). Recombinant MPP5 was efficiently immunoprecipitated by SN47 from cell lysates overproducing MPP5, whereas endogenous MPP5 was not (data not shown). By Western blot analysis we could not detect endogenous expression of CRB1 (data not shown). These results show that MPP4 interacts with MPP5 in the absence as well as presence of CRB1. To test for the presence of a protein complex containing MPP4 and CRB1, we used 293HEK cells overexpressing 3xFLAG-MPP4 and/or myc-CRB1. Anti-MPP4 antibody (AK4) immunoprecipitated MPP4 from 3xFLAG-MPP4-overproducing cell lines (Fig. 2E), and coimmu-

TABLE 2. Binding Energies (in kcal/mol) of Four SH3/GuK Module Combinations, Predicted from Homology Models

	GuK-Domain MPP4	GuK-Domain MPP5
SH3-Domain MPP4	147	118
SH3-Domain MPP5	144	137

noprecipitated CRB1 from cells overproducing 3xFLAG-MPP4 and myc-CRB1 (Fig. 2F), though at a much lower level.

In a reciprocal experiment, anti-myc antibody immunoprecipitated CRB1 from myc-CRB1 overproducing cell lines (data not shown), and coimmunoprecipitated MPP4 from cells overproducing 3xFLAG-MPP4 and myc-CRB1 at similar low levels (Fig. 2G). This result, as well as the anti-Flag immunoprecipitation of MPP4, indicates the presence of MPP4 and CRB1 in the same complex, though probably through endogenously expressed MPP5. The calculated size of CRB1 was 154 kDa, whereas CRB1 polyclonal antibodies recognized a protein >220 kDa on Western blot from 293HEK/CRB1 and MDCKII/CRB1 cells. The PROSITE program predicted 23 putative N-glycosylation sites (Swiss Institute of Bioinformatics). Therefore, we tested to see whether CRB1 is glycosylated in MDCKII/CRB1 cells. Incubation with tunicamycin shifted the molecular weight toward the expected 154 kDa (Fig. 2H), indicating extensive N-glycosylation of CRB1. The endogenous Crb1 from mouse retina[24] appears to be more than 220 kDa, whereas the calculated molecular weight is 153 kDa. This suggests that N-glycosylation also occurs in vivo in mouse retina.

Computer-Based Molecular Dynamics and In Vivo Interaction of Homo- and Heterodimers of MPP4 and -5

The interacting domains of MPP4 and -5 were analyzed by using a panel of deletion variants of both proteins in the yeast two-hybrid system (Fig. 3A, above dotted line). A fragment of MPP5 containing the SH3-HOOK region, flanked by strands A and D, specifically interacts with a fragment of MPP4 containing the GuK domain, flanked by strands E and F. When either of these strands was absent, the interaction was fully disrupted (data not shown). Furthermore, no interaction was found between the SH3-HOOK region of MPP5 and the full-size SH3-GuK module of MPP4, or between the full-length MPP5 and -4 proteins (data not shown). These results are analogous to the intra- and intermolecular interactions reported for the MAGUK protein PSD-95. In PSD-95, the interaction between the SH3 and GuK domains can either occur within a single peptide chain or between separate peptide chains. It has been proposed before that the interactions observed in PSD-95 are a conserved feature among MAGUK proteins.[45] A similar mechanism could thus be expected for MPP4/MPP5 based on our experimental results and the high percentage of sequence identity to PSD-95, especially at the domain interface. To analyze this possibility, we built 3D homology models of the SH3-GuK domains of MPP4 and -5 (Fig. 3B, left), based on the crystal structures of PSD-95.[39,45] All four permutations of domain interactions were analyzed: $MPP4^{SH3}$-$MPP4^{GuK}$, $MPP4^{SH3}$-$MPP5^{GuK}$, $MPP5^{SH3}$-$MPP4^{GuK}$, and $MPP5^{SH3}$-$MPP5^{GuK}$. In all cases, the domain interfaces were stabilized by salt bridges and hydrophobic interactions, most prominently by a conserved tyrosine (Y413 in MPP4 and Y466 in MPP5) that forms the core of the SH3 domain, but belongs to the E-strand just before the GuK domain (Fig. 3B, below dotted line). The domain binding energies of the four models are listed in Table 2.

The binding energies of the SH3-GuK modules of MPP4 and -5 are predicted according to the NOVA energy function (in kilocalories per mole). Results were obtained by subtracting the NOVA energy of the SH3/GuK complex from the energies of separated SH3 and GuK modules; higher energies thus indicate better binding. The highest binding energy (147 kcal/mol) is predicted for the SH3/GuK self-interaction in MPP4. This matches our experimental finding in the yeast two-hybrid system that a full-length MPP4 construct did not bind to MPP5 (data not shown), but obviously prefers the self-interaction. The second strongest binding energy was obtained for $MPP5^{SH3}$-$MPP4^{GuK}$. This model contains several salt bridges that are either missing or less pronounced in the remaining two models (Fig. 3B, right). Indeed, the $MPP5^{SH3}$-$MPP4^{GuK}$ interaction was the one we first discovered experimentally in the yeast two-hybrid screening (Fig. 3A).

To validate the model further, we analyzed the binding affinities of the SH3 and GuK domains in MPP4 and -5 (Fig. 3A, right). We were able to confirm in the sensitive liquid ONPG assay that the MPP4 domains interact more strongly than the ones in MPP5.

Expression of *CRB1*, *MPP5*, and *MPP4*

Expression analysis by semiquantitative RT-PCR on a panel of RNAs from several human tissues showed that *CRB1* is predominantly expressed in the retina. An increase in the number of PCR cycles identified a lower level of expression in brain, testis, and fetal eye (Fig. 4). *MPP5* is more ubiquitously expressed and is also present in the retina. *MPP4* is highly expressed in the retina. An increase in the number of PCR cycles identified a lower level of expression in brain, testis, ARPE cell line and fetal eye.

Low levels of MPP4 RNA were also detected in human retinal pigment epithelium, but MPP4 protein was below detection levels in human and mouse RPE.[24]

Immunolocalizations of CRB1, MPP4, and MPP5 in Human Retina

Immunohistochemistry and confocal laser scanning microscopy were used to determine the subcellular protein localiza-

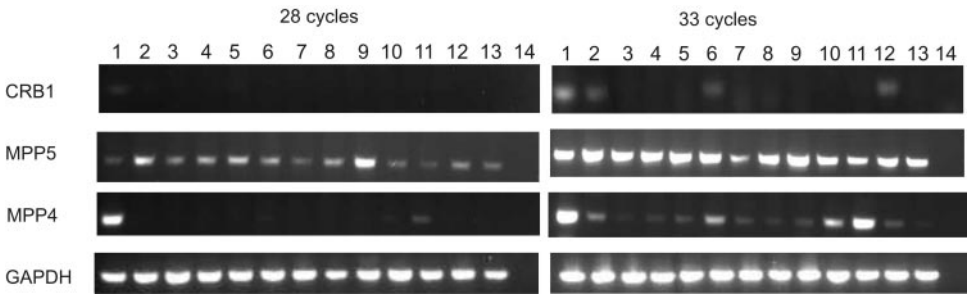

FIGURE 4. mRNA expression profiles of *CRB1*, *MPP5*, and *MPP4* in human tissues and an RPE cell line (ARPE) determined by RT-PCR. *Lane 1*: retina; *lane 2*: brain; *lane 3*: skeletal muscle; *lane 4*: heart; *lane 5*: lung; *lane 6*: testis; *lane 7*: kidney; *lane 8*: liver; *lane 9*: placenta; *lane 10*: ARPE; *lane 11*: RPE; *lane 12*: fetal eye; *lane 13*: fetal cochlea; and *lane 14*: negative water control. *GAPDH* served as a positive control.

tion of CRB1, MPP4, and MPP5. Anti-CRB1 antibodies AK2 and -5 detected CRB1 at the outer limiting membrane (OLM) of human retina. Using monoclonal antibodies against human β-catenin as a marker for the adherens junction, localization of CRB1 apical to the adherens junction was detected (Figs. 5A–D). Anti-MPP5 antibodies (SN47) detected the protein at the OLM, also apical to the AJ (Figs. 5E–H), where it colocalized with CRB1 (Figs. 5I–L). MPP4 was detected at the OLM and in the outer plexiform layer (OPL) of human retina with AK4 (and AK8) antibodies. At the OLM, MPP4 was detected apical to the adherens junction. However, the intensity of the signal at the OLM was much lower than the MPP4 staining intensity in the OPL (Figs. 5M–Q).

Ultrastructural Localization of Mouse Mpp4 in Retina

Mpp4 was detected with immunoelectron microscopy at the OLM and in the cone pedicles and rod spherules. At the OLM, Mpp4 was present apically to and at the adherens junction contacts (Figs. 6A, 6E). Staining was also detected at membranes of the Golgi area (Figs. 6A, asterisk, 6D) and other small and large vesicles in the inner segments of photoreceptors. In rod photoreceptors, there was a strong association of the signal with the lateral plasma membranes of the spherules (Figs. 6B, 6F). In the cones, the Mpp4 signal was concentrated at the basal side, which comprises the contacts with horizontal and bipolar cells and also at the lateral side of the pedicle plasma membrane (Figs. 6C asterisk, 6G). In both types of photoreceptors, Mpp4 staining was also associated with vesicles proximal to the presynaptic membrane.

The ultrastructural study showed that retinal Mpp4 is restricted to the photoreceptors. We did not detect any protein in the Müller (Fig. 6E), bipolar, horizontal, or other neuronal retinal cell types. This finding correlates with in situ hybridization analysis on mouse retina showing distribution of mRNA coding for Mpp4 protein in the photoreceptor inner segments and outer nuclear layer (ONL).[46,47] We conclude that Mpp4 is localized in rod and cone photoreceptors at the plasma membrane and at membranes of intracellular vesicles around the subapical region (SAR) and adherens junctions, and OPL.

Discussion

MPP4 as a Member of the CRB1 Protein Scaffold

Recent findings have emphasized the central role of CRB1 and its intracellular interactor MPP5/PALS1 in the regulation of epithelial polarity. However, the larger part of both CRB1, containing a putative FERM-binding motif, and MPP5, containing the additional MAGUK modules, have not yet been described to have a role in this process. The putative protein–protein-interacting capacity of these domains in any tissue was still to be shown. This motivated us to search for interactors with these specific domains in the retina by using a yeast two-hybrid approach. In this study, our results showed that the MAGUK protein MPP4 was recruited to the MPP5/CRB1 complex through direct binding of the SH3-GuK modules of both MPP family members. These three proteins form a multiprotein complex at the OLM of the retina. Using antibodies directed against the multiple PDZ protein Mupp1, we recently showed coimmunoprecipitation of endogenous Mpp4, Mpp5, and Crb1 from mouse retinal lysates of wild-type mice and coimmunoprecipitation of MPP4 and -5 from lysates of *Crb1* knockout mice.[24] We now have identified MPP4 as a binding partner for the SH3-HOOK region of MPP5.

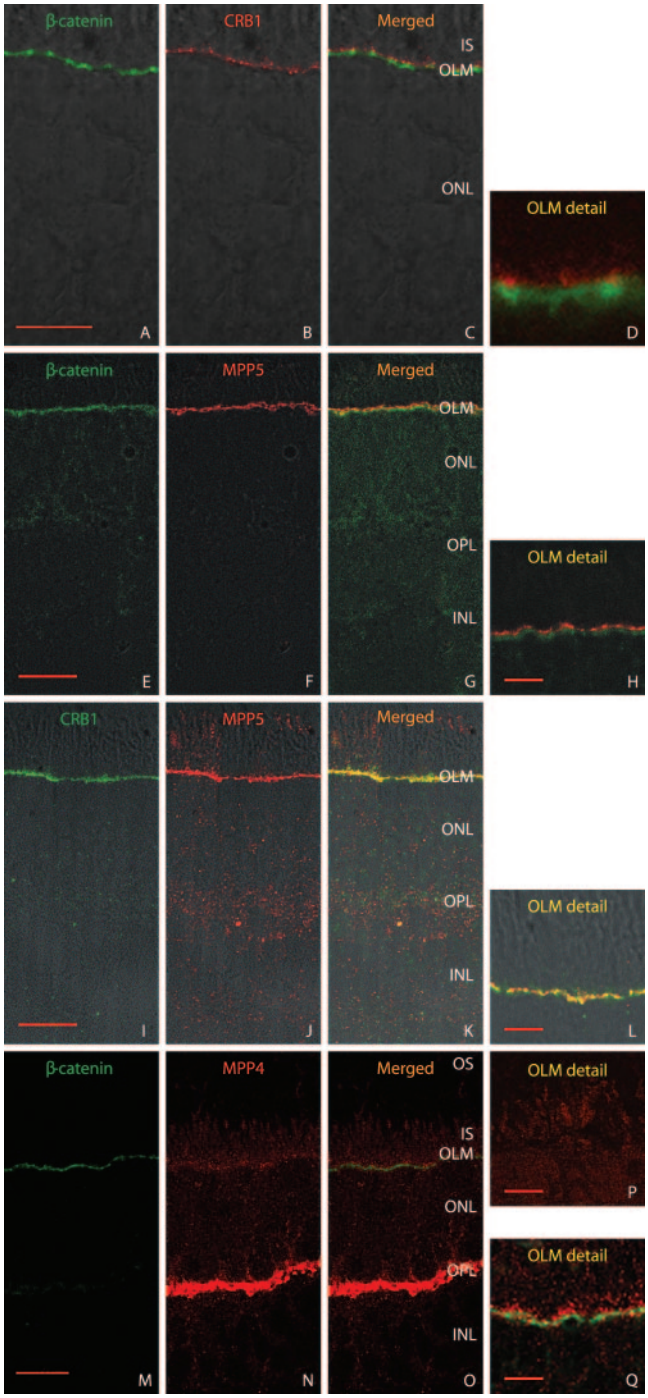

Figure 5. Distribution of MPP4, MPP5, CRB1, and β-catenin in adult human retina. Confocal images of human retinas stained with antibodies against β-catenin (**A**, **C**, **D**, **E**, **G**, **H**, **M**, **O**, **Q**), CRB1 (**B–D**, **I**, **K**, **L**), MPP5 (**F–H**, **J–L**), MPP4 (**N**, **O**, **Q**), or control secondary antibodies (**P**). Anti-β-catenin antibody strongly stained the adherens junction (**D**, **H**, **Q**), whereas anti-CRB1 antibody AK2 (**D**, L), anti-MPP5 SN47 (**H**, **L**), and anti-MPP4 AK4 (**N**, **O**, **Q**) stained the SAR in the OLM. MPP5 and CRB1 colocalized at the SAR (**L**). AK4 stained the OPL (**N**, **O**) and the OLM (**O**, **Q**), whereas secondary antibodies (**P**) produced some background staining in the photoreceptor inner and outer segments. IS, inner segments; ONL, outer nuclear layer; OPL, outer plexiform layer; OS, outer segments; INL, inner nuclear layer. Scale bars: (**A–C**, **H**, **L**, **P**, **Q**) 10 μm; (**D**, **E–G**, **I–K**, **M–O**) 20 μm.

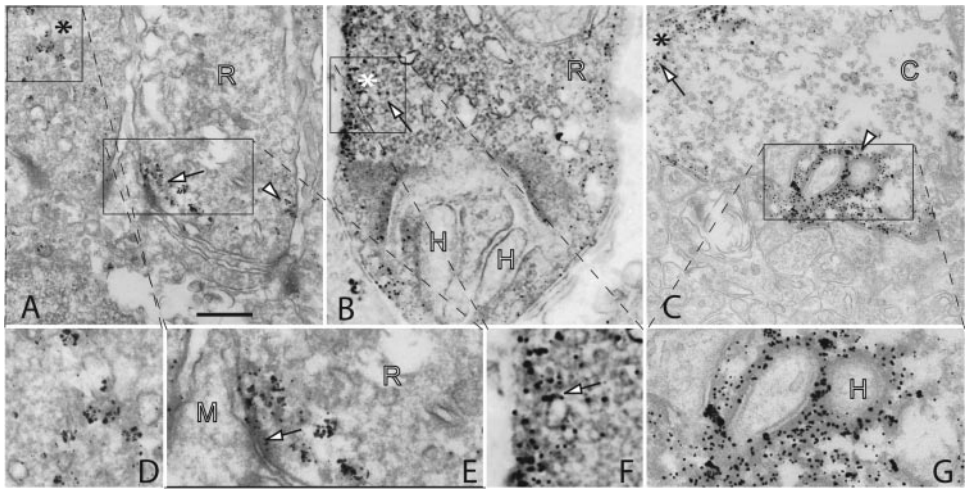

FIGURE 6. Immunoelectron microscopy of mouse Mpp4 in retina. (**A**) In the OLM, Mpp4 was located at the plasma membrane apical to and at the zonula adherens contacts (*arrowhead* and *arrow*, respectively). There was also staining of the trans-Golgi network (✶). (**B**) In rod photoreceptors, the lateral plasma membranes of the spherules were strongly stained (✶). Mpp4 staining was also found associated with vesicles proximal to the presynaptic membrane (*arrow*). (**C**) Mpp4 was found at the basal side of cone pedicles, where it concentrated at the contacts with horizontal cell processes and bipolar cell dendrites (*arrowhead*) and also at the plasma membrane of the lateral side of the pedicle membrane (✶). As in rods, Mpp4 staining was also associated with vesicles proximal to the presynaptic membrane (*arrow*). (**D**) Detailed view of the staining of the Golgi area in the inner segment of a rod. (**E**) Magnification of the adherens junction showing the presence of the signal at the photoreceptor side (*arrow*), not in the Müller glia cell. (**F**) MPP4 was located at the presynaptic plasma membrane and proximal vesicles (*arrow*). (**G**) At the cone synapse, the signal was associated with the presynaptic membrane. R, rod photoreceptor; C, cone photoreceptor; H, horizontal cell; M, Müller glia cell. Scale bar, 0.5 μm.

Mechanism of Interaction and Implications for Regulation

The interaction between MPP5 and -4 involves the C-terminal end of MPP4. Alternative interaction through L27 domain dimerization was excluded. In a yeast two-hybrid experiment, no L27 domain binding was found between MPP4 and -5, whereas the L27 domains of PATJ and MPP5 did show interaction (data not shown).

Detailed analysis revealed that the E and F strands flanking the GuK domain of MPP4 are essential for binding. This is in full agreement with the folding according to the crystal structure of PSD-95.[39,45] In PSD-95, the SH3-HOOK region interacts both in *cis* and *trans* with the E-GuK-F region in vitro. The intramolecular interaction initially prohibits intermolecular interactions by preventing a mechanism called 3D domain swapping. Domain swapping allows proteins to assemble dimers or higher order oligomers by exchanging complementary substructures.[48–50] The need of a cofactor or modulator has been postulated to switch the preference from intra- toward intermolecular interactions in vivo, thus enabling specific regulation of MAGUK multimerization at the cytoplasmic membrane.[39,45]

The 3D homology modeling of MPP5 and -4 pointed to a PSD-95-like interaction mechanism that also matched the results of our yeast two-hybrid binding assays. GST pull-down analysis and immunoprecipitation experiments both confirmed the interactions biochemically and provided in vivo evidence for the proposed regulatory mechanism of heterodimerization. The full-length proteins that were the targets for immunoprecipitation did coprecipitate the full complex of CRB1, MPP4, and MPP5 from HEK293 cells, indicating that in these cells the regulatory factor is present (Figs. 2C, 2D). Good candidates for regulation of the dimerization of MPP5 are members of the 4.1 protein family, as the variable hinge or HOOK region of MPP5 contains a conserved 4.1 binding motif. MPP4 does not contain this particular conserved motif in the same region, but does have a predicted α-helical stretch. We propose that regulation of dimerization of these MAGUK proteins is one of the factors that governs a dynamic variation of proteins that are present at this polarity-associated protein scaffold.

SH3 domains of tyrosine kinases are usually involved in protein–protein interactions by binding to proline-rich sequences,[51,52] and have been described to couple substrates to enzymes, thereby regulating enzymatic activities.[53] However, based on the 3D homology models presented herein and the interactions identified in this study, the SH3 module of MPP4 and -5 seems to be functionally different from the conventional ones. The SH3 domain of MPP5 interacts with the GuK domain of MPP4 as well as with its own GuK domain.

Distribution of Protein Expression in the Human Retina

Whereas MPP5 is expressed ubiquitously,[7] both *CRB1* and *MPP4* genes are expressed more selectively in eye and brain.[54] *MPP4* RNA is also present in liver, spleen, heart,[46,47,54,55] and testis, but at much lower levels. Previous experiments showed that *Crb1* and *Mpp4* RNA is expressed in the ONL and inner photoreceptor segments of the retina.[46,54] *Crb1* RNA was also detected at low levels in the inner nuclear layer.

The protein complex CRB1-MPP5-MPP4 localizes subapically to the adherens junction at the OLM of the retina. The localization of Mpp4/MPP4, Mpp5/ MPP5, and Crb1/CRB1 appears to be conserved between mice and humans.[24] Our results on MPP4 localization partially overlap with the positioning described for MPP4 in mouse retina.[47] Differences in genetic background or detection level may explain why Mpp4 was not detected in cones or OLM in previous studies[47] and may explain the localization of MPP4 in the connecting cilia of bovine and porcine.[56]

We observed that Mpp4 is detected at intracellular vesicles and at the plasma membrane. Mpp4 is also located at the presynaptic membrane and proximal vesicles. The localization of MPP4 at more than one functionally different cell structure suggests participation in different protein complexes. Some MAGUK proteins target and anchor glutamate receptors to the synaptic terminals.[57] It has been proposed that the complex involving the MAGUK protein CASK acts as a nucleation site for the assembly of proteins involved in synaptic vesicle exocytosis and synaptic junctions.[58,59] It is tempting to speculate on possible functions of MPP4 in vesicle targeting or fusion complexes at the photoreceptor synapses and the region apical to the adherens junction.

Implications for Inherited Retinal Degenerations

Altogether, these facts provide strong evidence for the involvement of CRB1, MPP5, and MPP4 in a common pathway that determines the polarity of photoreceptors in the retina. Based on the recruitment of both MPP4 and -5 to the CRB1 protein scaffold, the disruption of retinal lamination observed with loss of mouse Crb1[24] and the zebra fish MPP5 homologue *Nagie oko*[14] and the high expression of MPP4 in the retina, we propose that *MPP5* and *MPP4* are functional candidate genes for inherited retinal degenerations.

The *MPP4* gene has been screened for mutations in RP with 300 patients, and it was mapped in a locus for autosomal recessive retinitis pigmentosa (RP26 locus) at 2q31-33, but no mutations were identified. Recently, mutations in the neighboring *CERKL* gene were found to cause RP26.[60] However, based on the more severe phenotype that is often observed in patients with mutations in *CRB1*, *MPP4* remains a candidate gene for similar eye disorders. Mutational changes in members of the complex that are closely linked could lead to a similar disrupting effect of the protein complex in the retina. Mutation analysis in selected patient panels could reveal the involvement of either *MPP4* or *MPP5* in inherited retina disorders.

Acknowledgments

The authors thank Willem Kamphuis and Serge van de Pavert for advice and critical discussions on the immunohistochemical data; Anna Malysheva, Jan Meuleman, and Paulus de Jong for comments on the manuscript; and Maarten L. Arends for excellent technical assistance.

References

1. Kowalczyk AP, Moses K. Photoreceptor cells in flies and mammals: crumby homology? *Dev Cell*. 2002;2:253–254.
2. Altschuler Y, Hodson C, Milgram SL. The apical compartment: trafficking pathways, regulators and scaffolding proteins. *Curr Opin Cell Biol*. 2003;15:423–429.
3. Fanning AS, Jameson BJ, Jesaitis LA, Anderson JM. The tight junction protein ZO-1 establishes a link between the transmembrane protein occludin and the actin cytoskeleton. *J Biol Chem*. 1998; 273:29745–29753.
4. Itoh M, Furuse M, Morita K, et al. Direct binding of three tight junction-associated MAGUKs, ZO-1, ZO-2, and ZO-3, with the COOH termini of claudins. *J Cell Biol*. 1999;147:1351–1363.
5. Anderson JM. Cell signalling: MAGUK magic. *Curr Biol*. 1996;6: 382–384.
6. Woods DF, Bryant PJ. The discs-large tumor suppressor gene of Drosophila encodes a guanylate kinase homolog localized at septate junctions. *Cell*. 1991;66:451–464.
7. Kamberov E, Makarova O, Roh M, et al. Molecular cloning and characterization of Pals, proteins associated with mLin-7. *J Biol Chem*. 2000;275:11425–11431.
8. Gumbiner B, Lowenkopf T, Apatira D. Identification of a 160-kDa polypeptide that binds to the tight junction protein ZO-1. *Proc Natl Acad Sci USA*. 1991;88:3460–3464.
9. Gonzalez-Mariscal L, Betanzos A, Avila-Flores A. MAGUK proteins: structure and role in the tight junction. *Semin Cell Dev Biol*. 2000;11:315–324.
10. Roh MH, Makarova O, Liu CJ, et al. The Maguk protein, Pals1, functions as an adapter, linking mammalian homologues of Crumbs and Discs Lost. *J Cell Biol*. 2002;157:161–172.
11. Leonoudakis D, Conti LR, Anderson S, et al. Protein trafficking and anchoring complexes revealed by proteomic analysis of inward rectifier potassium channel (Kir2.x)-associated proteins. *J Biol Chem*. 2004;279:22331–22346.
12. Dimitratos SD, Woods DF, Stathakis DG, Bryant PJ. Signaling pathways are focused at specialized regions of the plasma membrane by scaffolding proteins of the MAGUK family. *Bioessays*. 1999;21: 912–921.
13. Knust E, Tepass U, Wodarz A. crumbs and stardust, two genes of Drosophila required for the development of epithelial cell polarity. *Dev Suppl*. 1993;261–268.
14. Wei X, Malicki J. Nagie oko, encoding a MAGUK-family protein, is essential for cellular patterning of the retina. *Nat Genet*. 2002; 150–157.
15. Izaddoost S, Nam SC, Bhat MA, Bellen HJ, Choi KW. Drosophila Crumbs is a positional cue in photoreceptor adherens junctions and rhabdomeres. *Nature*. 2002;416:178–183.
16. Pellikka M, Tanentzapf G, Pinto M, et al. Crumbs, the Drosophila homologue of human CRB1/RP12, is essential for photoreceptor morphogenesis. *Nature*. 2002;416:143–149.
17. Hong Y, Ackerman L, Jan LY, Jan YN. Distinct roles of Bazooka and Stardust in the specification of Drosophila photoreceptor membrane architecture. *Proc Natl Acad Sci USA*. 2003;100:12712–12717.
18. Hong Y, Stronach B, Perrimon N, Jan LY, Jan YN. Drosophila Stardust interacts with Crumbs to control polarity of epithelia but not neuroblasts. *Nature*. 2001;414:634–638.
19. Grawe F, Wodarz A, Lee B, Knust E, Skaer H. The Drosophila genes crumbs and stardust are involved in the biogenesis of adherens junctions. *Development*. 1996;122:951–959.
20. Wodarz A, Hinz U, Engelbert M, Knust E. Expression of crumbs confers apical character on plasma membrane domains of ectodermal epithelia of Drosophila. *Cell*. 1995;82:67–76.
21. Tepass U, Theres C, Knust E. Crumbs encodes an EGF-like protein expressed on apical membranes of Drosophila epithelial cells and required for organization of epithelia. *Cell*. 1990;61:787–799.
22. Bachmann A, Schneider M, Theilenberg E, Grawe F, Knust E. Drosophila Stardust is a partner of Crumbs in the control of epithelial cell polarity. *Nature*. 2001;414:638–643.
23. Makarova O, Roh MH, Liu CJ, Laurinec S, Margolis B. Mammalian Crumbs3 is a small transmembrane protein linked to protein associated with Lin-7 (Pals1). *Gene*. 2003;302:21–29.
24. Van de Pavert SA, Kantardzhieva A, Malysheva A, et al. Crumbs homologue 1 is required for maintenance of photoreceptor cell polarization and adhesion during light exposure. *J Cell Sci*. 2004; 117:4169–4177.
25. den Hollander AI, ten Brink JB, de Kok YJM, et al. Mutations in a human homologue of Drosophila crumbs cause retinitis pigmentosa (RP12). *Nat Genet*. 1999;23:217–221.
26. Lotery AJ, Jacobson SG, Fishman GA, et al. Mutations in the CRB1 gene cause Leber congenital amaurosis. *Arch Ophthalmol*. 2001; 119:415–420.
27. den Hollander AI, Heckenlively JR, van den Born LI, et al. Leber congenital amaurosis and retinitis pigmentosa with Coats-like exudative vasculopathy are associated with mutations in the crumbs homologue 1 (CRB1) gene. *Am J Hum Genet*. 2001;69:198–203.
28. Bernal S, Calaf M, Garcia-Hoyos M, et al. Study of the involvement of the RGR, CRPB1, and CRB1 genes in the pathogenesis of autosomal recessive retinitis pigmentosa. *J Med Genet*. 2003;40: E89.
29. Lotery AJ, Malik A, Shami SA, et al. CRB1 mutations may result in retinitis pigmentosa without para-arteriolar RPE preservation. *Ophthalmic Genet*. 2001;22:163–169.
30. Mehalow AK, Kameya S, Smith RS, et al. CRB1 is essential for external limiting membrane integrity and photoreceptor morphogenesis in the mammalian retina. *Hum Mol Genet*. 2003;12:2179–2189.
31. Meuleman J, Van de Pavert SA, Wijnholds J. Crumbs homologue 1 in polarity and blindness. *Biochem Soc Trans*. 2004;32:828–830.
32. Guan KL, Dixon JE. Eukaryotic proteins expressed in Escherichia coli: an improved thrombin cleavage and purification procedure of fusion proteins with glutathione S-transferase. *Anal Biochem*. 1991;192:262–267.
33. Fromont-Racine M, Rain JC, Legrain P. Building protein-protein networks by two-hybrid mating strategy: guide to yeast genetics and molecular and cell biology. *Methods Enzymol*. 2002;350:513–524.
34. Roepman R, Schick D, Ferreira PA. Isolation of retinal proteins that interact with retinitis pigmentosa GTPase regulator by interaction trap screen in yeast. *Methods Enzymol*. 2000;316:688–704.

35. Frangioni JV, Neel BG. Solubilization and purification of enzymatically active glutathione S-transferase (pGEX) fusion proteins. *Anal Biochem*. 1993;210:179–187.
36. den Hollander AI, van Driel MA, de Kok YJM, et al. Isolation and mapping of novel candidate genes for retinal disorders using suppression subtractive hybridization. *Genomics*. 1999;58:240–249.
37. Klooster J, Vrensen GF. The ultrastructure of the olivary pretectal nucleus in rats: a tracing and GABA immunohistochemical study. *Exp Brain Res*. 1997;114:51–62.
38. Kelley LA, MacCallum RM, Sternberg MJE. Enhanced genome annotation using structural profiles in the program 3D-PSSM. *J Mol Biol*. 2000;299:499–520.
39. McGee AW, Dakoji SR, Olsen O, et al. Structure of the SH3-guanylate kinase module from PSD-95 suggests a mechanism for regulated assembly of MAGUK scaffolding proteins. *Mol Cell*. 2001;8:1291–1301.
40. Rost B. Twilight zone of protein sequence alignments. *Protein Eng*. 1999;12:85–94.
41. Vriend G. What If: a molecular modeling and drug design program. *J Mol Graph*. 1990;8:52–56.
42. Chinea G, Padron G, Hooft RWW, Sander C, Vriend G. The use of position-specific rotamers in model-building by homology. *Proteins Struct Funct Genet*. 1995;23:415–421.
43. Krieger E, Koraimann G, Vriend G. Increasing the precision of comparative models with YASARA NOVA: a self-parameterizing force field. *Proteins Struct Funct Genet*. 2002;47:393–402.
44. Krieger E, Geretti E, Brandner B, et al. A structural and dynamic model for the interaction of interleukin-8 and glycosaminoglycans: support from isothermal fluorescence titrations. *Proteins*. 2004; 54:768–775.
45. Tavares GA, Panepucci EH, Brunger AT. Structural characterization of the intramolecular interaction between the SH3 and guanylate kinase domains of PSD-95. *Mol Cell*. 2001;8:1313–1325.
46. Conte I, Lestingi M, den Hollander AI, et al. Characterization of MPP4, a gene highly expressed in photoreceptor cells, and mutation analysis in retinitis pigmentosa. *Gene*. 2002;297:33–38.
47. Li M, Zhang SS, Barnstable CJ. Developmental and tissue expression patterns of mouse Mpp4 gene. *Biochem Biophys Res Commun*. 2003;307:229–235.
48. Bennett MJ, Schlunegger MP, Eisenberg D. 3D domain swapping: a mechanism for oligomer assembly. *Protein Sci*. 1995;4:2455–2468.
49. Schlunegger MP, Bennett MJ, Eisenberg D. Oligomer formation by 3D domain swapping: a model for protein assembly and misassembly. *Adv Protein Chem*. 1997;50:61–122.
50. Newcomer ME. Trading places. *Nat Struct Biol*. 2001;8:282–284.
51. Ren R, Mayer BJ, Cicchetti P, Baltimore D. Identification of a ten-amino acid proline-rich SH3 binding site. *Science*. 1993;259: 1157–1161.
52. Musacchio A, Saraste M, Wilmanns M. High-resolution crystal structures of tyrosine kinase SH3 domains complexed with proline-rich peptides. *Nat Struct Biol*. 1994;1:546–551.
53. Cohen GB, Ren R, Baltimore D. Modular binding domains in signal transduction proteins. *Cell*. 1995;80:237–248.
54. den Hollander AI, Ghiani M, de Kok YJM, et al. Isolation of Crb1, a mouse homologue of Drosophila crumbs, and analysis of its expression pattern in eye and brain. *Mech Dev*. 2002;110:203–207.
55. Stohr H, Weber BH. Cloning and characterization of the human retina-specific gene MPP4, a novel member of the p55 subfamily of MAGUK proteins. *Genomics*. 2001;74:377–384.
56. Stohr H, Stojic J, Weber BH. Cellular localization of the MPP4 protein in the mammalian retina. *Invest Ophthalmol Vis Sci*. 2003; 44:5067–5074.
57. Colledge M, Dean RA, Scott GK, et al. Targeting of PKA to glutamate receptors through a MAGUK-AKAP complex. *Neuron*. 2000; 27:107–119.
58. Butz S, Okamoto M, Sudhof TC. A tripartite protein complex with the potential to couple synaptic vesicle exocytosis to cell adhesion in brain. *Cell*. 1998;94:773–782.
59. Zhang Y, Luan Z, Liu A, Hu G. The scaffolding protein CASK mediates the interaction between rabphilin3a and beta-neurexins. *FEBS Lett*. 2001;497:99–102.
60. Tuson M, Marfany G, Gonzalez-Duarte R. Mutation of CERKL, a novel human ceramide kinase gene, causes autosomal recessive retinitis pigmentosa (RP26). *Am J Hum Genet*. 2004;74:128–138.